

Glycopolymers

Inhibition of *S. aureus* Infection of Human Umbilical Vein Endothelial Cells (HUVECs) by Trehalose- and Glucose-Functionalized Gold Nanoparticles

Yimeng Li, Nicholas Ariotti, Behnaz Aghaei, Elvis Pandzic, Sylvia Ganda, Mark Willcox, Manuel Sanchez-Felix, and Martina Stenzel*

Abstract: Microbial adhesion to host cells represents the initial step in the infection process. Several methods have been explored to inhibit microbial adhesion including the use of glycopolymers based on mannose, galactose, sialic acid and glucose. These sugar receptors are, however, abundant in the body, and are not unique to bacteria. Trehalose, in contrast, is a unique disaccharide that is widely expressed by microbes. This carbohydrate has not yet been explored as an anti-adhesive agent. Herein, gold nanoparticles (AuNPs) coated with trehalose-based polymers were prepared and compared to glucose-functionalized AuNPs and examined for their ability to prevent binding to endothelial cells. Acting as anti-adhesive agents, trehalose-functionalized NPs decreased the binding of *S. aureus* to HUVECs, while outperforming the control NPs. Microscopy revealed that trehalose-coated NPs bound strongly to *S. aureus* compared to the controls. In conclusion, nanoparticles based on trehalose could be a non-toxic alternative to inhibit *S. aureus* infection.

Anti-adhesion treatment has emerged as a promising anti-infection strategy due to the global emergency of antibiotics

resistance. For pathogenic invasion to occur, pathogens must first adhere to host cells. Anti-adhesion treatment inhibits the invasion of pathogens by preventing the adherence of pathogens with host cells. Unlike conventional antibiotic treatment, anti-adhesion treatment is less susceptible to antibacterial resistance.^[1] Adhesion can often occur via lectin-glycan interactions. Lectins are a type of protein located on the surface of cells and functions by binding to specific glycans.^[2] Glycomimetics have been employed as anti-adhesive that block interactions with lectins.^[3] In particular, well-defined macrostructures of the glycomimetics are attractive. Owing to the rapid development of nanotechnology, well-defined glycopolymers can be synthesized with proper functional groups, sizes and morphologies.^[4–6] As a result, glycopolymers have attracted interest as potent glycomimetic candidates that could serve as anti-adhesive.^[3,7,8]

A number of factors have been investigated in the synthesis of anti-adhesives including scaffolds, multivalency and size.^[5,9,10] Notably, the glycan specificity to lectins plays a crucial role in the binding behavior. For instance, the hemagglutinin of Influenza virus and Cholera toxins are well-known sialic acid-binding lectins.^[11] FimH of certain strain of pathogenic *E. coli* is a mannose-specific lectin.^[12] Human lectin Dendritic Cell-Specific Intercellular adhesion molecule-3-Grabbing Non-integrin (DC-SIGN), the target of HIV, is capable of specifically binding mannose and fucose.^[13,14] Accordingly, numerous glycopolymers employing different sugars, such as mannose, galactose, sialic acid and glucose, have been investigated depending on the targeted pathogens.^[7,10,15–20] However, diverse sugar receptors are also abundant in human cells, such as the expression of mannose receptors in liver and macrophage cells as well as sialic acid receptor on endothelial cells and leukocytes.^[11,21] These sugars on human cells play significant biological roles as they participate in multiple biological events other than adhesion. Therefore, promising inhibitors for anti-adhesion treatments are expected to possess the ability to bind specifically to bacteria but does not interfere with host systems.

Trehalose is a non-reducing disaccharide composed from two D-glucose molecules. As a result of its distinctive structure, trehalose displays impressive physical and chemical properties; including having high hydrophilicity and chemical stability.^[22] Trehalose is able to improve cell tolerance against extreme conditions, such as temperature and pH change. Inspired by its bio-functional role, trehalose-based polymers

[*] Y. Li, Dr. S. Ganda, Prof. M. Stenzel

Centre for Advanced Macromolecular Design, School of Chemistry, University of New South Wales Sydney, NSW 2052 (Australia)
E-mail: m.stenzel@unsw.edu.au

Dr. N. Ariotti
Electron Microscope Unit, Mark Wainwright Analytical Centre, University of New South Wales, Sydney, NSW 2052 (Australia)

Dr. B. Aghaei
Inventia Life Science Pty Ltd Sydney, NSW 2015 (Australia)
and

School of Biotechnology and Biomolecular Sciences, University of New South Wales, Sydney, NSW 2052 (Australia)

Dr. E. Pandzic
Katharina Gaus Light Microscopy Facility, Mark Wainwright Analytical Centre, University of New South Wales, Sydney, NSW 2052 (Australia)

Prof. M. Willcox
School of Optometry and Vision Science, University of New South Wales, Sydney, NSW 2052 (Australia)

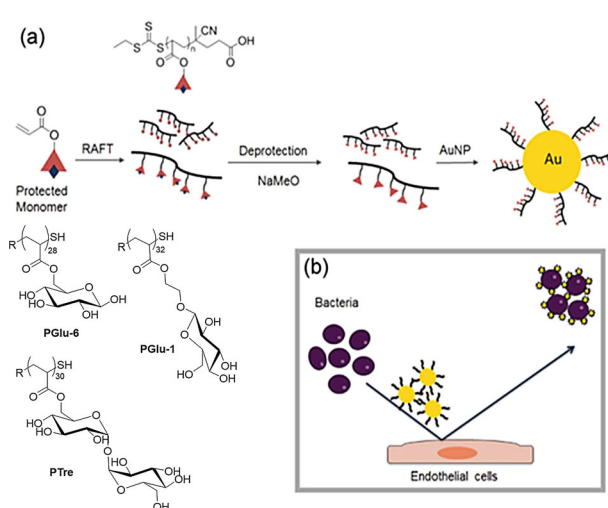
Dr. M. Sanchez-Felix
Novartis Institutes for BioMedical Research Cambridge, MA 02139 (USA)

 Supporting information and the ORCID identification number(s) for the author(s) of this article can be found under:
 <https://doi.org/10.1002/anie.202106544>

have been employed in the effort to protect, stabilize and even deliver proteins and nucleic acid.^[23–25] Notably, trehalose occurs in prokaryotes, lower eukaryotes, plants and invertebrates.^[26] The biosynthesis of trehalose is absent in mammals. However, the specific hydrolytic enzyme trehalase is expressed in the microvillus of the intestinal mucosa and renal brush border membrane in humans.^[27] Trehalose is a fundamental carbohydrate in bacteria, not only as energy source. Trehalose dimycolate is a glycolipid that exists in the cell wall of *Mycobacterium tuberculosis*.^[28] This trehalose derivative specifically binds to the C-type lectin (Mincle) on macrophages and mediates bacterial adhesion.^[29] Accordingly, trehalose-based nanoparticles have been developed to detect mycobacteria.^[30,31] As trehalose glycopolymers are non-toxic to mammalian cells,^[25,32,33] these polymers could potentially be used in infection treatments, particularly in anti-adhesion treatment.

Herein, we explored the potential role of trehalose-based nanoparticles as an anti-adhesive, to prevent adhesion of bacteria to endothelial cells. Three glyco-gold nanoparticles (glyco-AuNP) and their performance as inhibitors of bacterial infections is described and investigated. As trehalose is a disaccharide based on two α -glucose, connected by 1,1-glycosidic bond, we choose to use glycopolymers based on glucose as control. In these glycopolymers, the glucose was conjugated to the polymer backbone either in C1 or C6 position. While other glycopolymers can be used as control, we try to specifically answer the question if the disaccharide structure is essential or if one glucose unit is sufficient. Therefore, AuNPs were coated with different glycopolymers (Scheme 1) and the resulting glyco-AuNPs were evaluated in regard to their cell toxicity, action as anti-adhesives and their binding to bacteria.

The synthetic strategy to the glycopolymers and detailed discussed on the synthesis can be found in the supporting information. Protected C1 and C6 functionalized glucoside monomers and trehalose monomer were synthesized based on previously published procedures,^[34–36] (ESI, Figure S1–S4).



Scheme 1. a) Schematic illustration of the synthesis of glyco-AuNPs and b) schematic representation of anti-adhesion function of glyco-AuNPs.

Acrylate-based monomers were polymerized via RAFT polymerization resulting in homoglycopolymers with similar degree of polymerizations (DP) of 30 (ESI, Table S1, Figure S9), followed by deprotection (ESI, Figure S6–S8).

AuNPs were synthesized via the seeded-growth method based on previous work.^[37] To evaluate the effect of nanoparticle (NP) size on inhibition of adhesion, AuNPs of two different sizes, 62 nm (Au_{62}NP) and 16 nm (Au_{16}NP), were prepared and analyzed with transmission electron microscopy (TEM) (Figure 1a and b, ESI, Figure S10). The resulting AuNPs were coated with the prepared glycopolymers via thiol-gold interaction by mixing glycopolymers with AuNPs in water. UV/Vis analysis revealed a red shift (from 537 nm to 539 nm) confirming the successful polymer grafting (Figure 1c). The increase of the AuNP size after coating was observed by dynamic light scattering (DLS) measurement (Figure 1d, ESI, Table S2), and the zeta potential of all AuNPs ranged between -25 mV and -30 mV, most likely due to the carboxylic group of the R-group of the RAFT agent. The negative charge can assist in repelling the adsorption of blood proteins. In addition, thermal gravimetric analysis (TGA) was employed to measure the grafting density of glyco-AuNPs (ESI, Figure S11 and Table S3). In general, the measured grafting densities ranged from 0.17 to 0.37 chain per nm^2 with PGlu-6 displaying the highest grafting density whilst PTre displayed the lowest grafting density. Although the chain lengths of the three glycopolymers were similar, the molecular weights of the glycopolymers were different and hence the bulkier side groups led to a reduced grafting density.

Endothelial cells function as a physical barrier between blood and tissue and the ability of microbes to adhere to them plays a significant role in a number of infection pathogenesis.^[38] For example, bacterial adhesion to endocardial surfaces results in acute infective endocarditis.^[39] Therefore, HUVECs were chosen as the host cells in this project.

Prior to studying the ability of nanoparticles to prevent adhesion, the cytotoxicity of three 62 nm glyco-AuNPs were

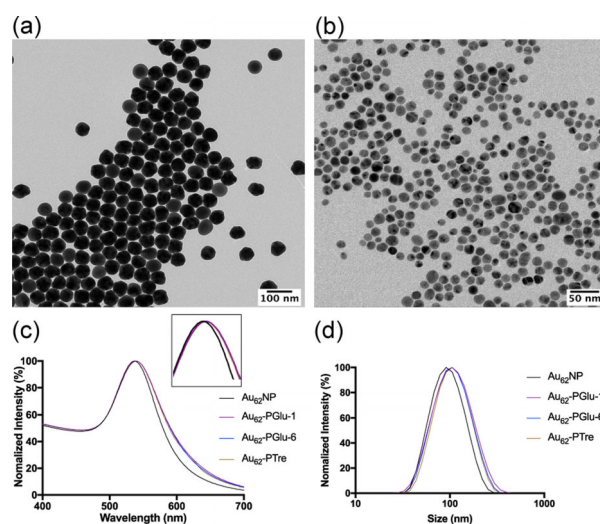


Figure 1. TEM images of a) Au_{62}NP and b) Au_{16}NP . c) UV/Vis spectra of uncoated Au_{62}NP and coated glyco-AuNPs. d) Size increase of uncoated Au_{62}NP and coated glyco-AuNPs as measured by DLS.

evaluated by WST-1 assay using two healthy cell lines: mouse macrophage RAW 264.7 and human umbilical vein endothelial cells (HUVECs). After 48 h incubation with glyco-AuNPs, the cytotoxicity against RAW 264.7 and HUVECs was determined (ESI, Figure S12). At concentrations up to 0.75 mg mL^{-1} , none of the tested glyco-AuNPs displayed significant toxicity to these cell lines. In fact, glyco-AuNPs appeared to enhance the proliferation of RAW 264.7 cells in the range from 0.19 mg mL^{-1} to 0.75 mg mL^{-1} . Although glycopolymers, including trehalose-based polymers, are often considered non-toxic,^[24,40,41] high levels of toxicity is occasionally observed by trehalose-based materials such as nanoparticles prepared from trehalose 6,6'-dimycolate.^[42] Based upon the cytotoxicity results, the highest concentration of glyco-AuNPs used in the following bio-work was set to 0.6 mg mL^{-1} .

Gram-positive bacteria *Staphylococcus aureus* 38 served as the infecting bacteria, as *S. aureus* is known to strongly adhere to HUVECs.^[43] The Gram-negative bacteria *Pseudomonas aeruginosa* PAO1 was used as a further model. To better understand the efficiency of glyco-AuNPs as anti-adhesives, flow cytometry was used as a quantitative technique.^[44] In this established technique, the host cells and bacteria are stained separately to determine their co-localization. HUVECs and bacteria were stained with Hoechst 33342 and Vybrant™ DiD, respectively, before co-incubation for 2 h with nanoparticles. Afterwards, unbound bacteria and nanoparticles were removed from the HUVECs by washing with Hank's balanced salt solution (HBSS). The monolayer of cells was trypsinized and collected for flow cytometry. The measured median fluorescence intensity (MFI) of DiD was correlated directly to the level of bacterial infection. A sample that was not treated with nanoparticles and a sample containing only HUVECs were employed as control and background, respectively. The MFI of the background was subtracted from the MFI of the control sample, and this was regarded as 100% infection. The presence of nanoparticles is expected to decrease the MFI if they inhibit infection. A multiplicity of infection (MOI), the ratio of bacteria to HUVECs, was kept at 50:1.

All three 62 nm glyco-AuNPs were evaluated at concentrations of 0.15 mg mL^{-1} , 0.3 mg mL^{-1} and 0.6 mg mL^{-1} using the *S. aureus*—HUVEC system. It is evident from Figure 2a that the percentage of co-associated cells decreased with an increasing amount of nanoparticles (ESI, Table S4). Most notable is the inhibition by Au₆₂-PTre which reduced the association to $54.9 \pm 10.9\%$ at a concentration of 0.6 mg mL^{-1} . Interestingly, Au-PGlu-6 and Au-PTre were both capable in inhibiting infection, however, the underlying mechanism as to how this occurs remains unclear. Bacteria use carbohydrates in a range of ways and also have means of taking up trehalose.^[45] In the case of *S. aureus* this bacterium has a large amount of carbohydrate transporters, including several phosphotransferase system (PTS) transporters, ATP-binding cassette (ABC) transporters and others, which distinguishes it from other *Staphylococcus* types.^[46,47] These transporters make it possible to metabolize an array of sugars as many transporters are not specific to one type of sugar. Therefore, a possible mechanism for the observed inhibition

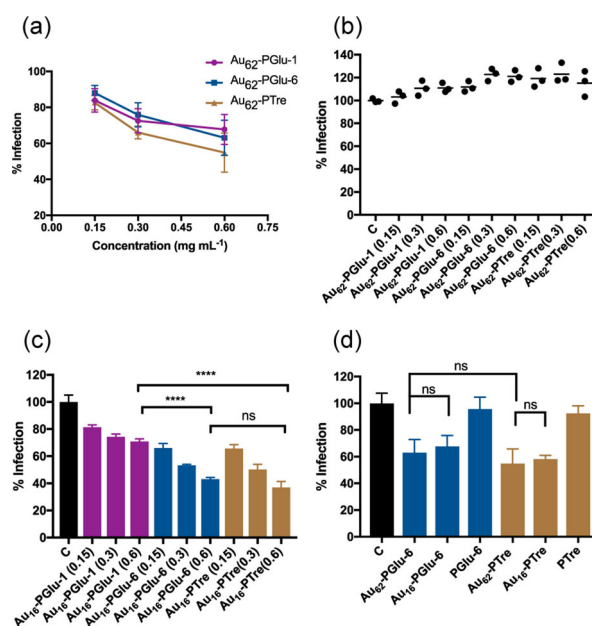


Figure 2. Inhibition of adhesion of bacteria to HUVECs by glyco-AuNPs. a) Inhibition of *S. aureus* 38 infection with 62 nm glyco-AuNPs at 0.15, 0.3, 0.6 mg mL^{-1} . b) Inhibition of *P. aeruginosa* PAO1 infection by 62 nm glyco-AuNPs at 0.15, 0.3, 0.6 mg mL^{-1} . c) Inhibition of *S. aureus* 38 infection by 16 nm glyco-AuNPs at 0.15, 0.3, 0.6 mg mL^{-1} . d) Inhibition of *S. aureus* 38 infection using glyco-AuNPs and unconjugated glycopolymers with equivalent glycopolymer contents (PGlu-6, 1.8 μM ; PTre, 0.8 μM). (C represents control sample containing HUVEC and bacteria.) Data shown as mean \pm SD; **** $P < 0.0001$. All P values were from one-way ANOVA followed by Turkey's multiple comparisons tests.

may be the interaction of transporters in the surface of *S. aureus*. This may include ABC permease LpqY/SugABC which is specific to trehalose,^[48] or other trehalose PTS permease (TreB) which also act as trehalose transporters in Gram-positive bacteria.^[49,50] Moreover, some surface-associated enzymes involved in the carbohydrate metabolism^[51] can interact with trehalose.^[52,53]

Similarly, the effects of glyco-AuNPs on inhibiting adhesion were studied on Gram-negative bacteria, using *P. aeruginosa* PAO1 as a model (Figure 2b). In this case, no signs of inhibition were observed for any nanoparticles at concentrations up to 0.6 mg mL^{-1} . This implies a lack of nanoparticle binding interaction with *P. aeruginosa*. While it can only be speculated as to why *P. aeruginosa* does not respond to the presence of glyco-AuNPs, there are significant differences in the structure of transporter molecules between Gram-negative and Gram-positive bacteria. For example, the trehalose-specific LpqY/SugABC transporter has a substrate binding protein (SBP), LpqY, on the bacterial surface. In Gram-positive bacteria *Mycobacterium smegmatis* (*M. smegmatis*), the arrangement of LpqY (SBP) is significantly different relative to the rest of the transporter and to the SBPs found on Gram-negative *E. coli*.^[54] Furthermore, Gram-negative bacteria possess an outer membrane in the cell wall, a feature which is not displayed by Gram-positive bacteria. This outer membrane may also be suspected to hinder the interaction of nanoparticles with certain transporters.^[50] The

outer membrane proteome of *P. aeruginosa* PAO1 has a glucoside-sensitive porin but there is no evidence of surface-associated enzymes involved in carbohydrate metabolism.^[55]

Next, the inhibitory effect of *S. aureus* adhesion by the 16 nm glyco-AuNPs was studied to evaluate the effect of the nanoparticle size (Figure 2c). Interestingly, Au₁₆-PGlu-6 and Au₁₆-PTre led to similar inhibition effects (43.2 ± 1.2% and 36.9 ± 4.4% infection) at 0.6 mg mL⁻¹ while Au₁₆-PGlu-1 resulted to weak inhibition (71.0 ± 1.8% infection). Au₁₆-PGlu-6 and Au₁₆-PTre clearly showed a trend in concentration-dependent inhibition. This result confirmed that the activity of the inhibitors is dependent on the substitution position of sugar. Glycopolymers with glucose modified on the C6 position is significantly more effective as inhibitors than the analogues based on substitution at the C1 position.

Furthermore, at same NP concentrations, the smaller NPs Au₁₆-PGlu-6 and Au₁₆-PTre appear to display stronger inhibition capacity than their larger-sized counterparts. This is however deceiving as the size of the NPs are now smaller, and therefore more nanoparticles and a higher fraction of glycopolymers are present at the same concentration in mg mL⁻¹ (Table 1). Also, variations in grafting densities need to be taken into account that may lead to different amounts of sugar per AuNP. Although Au-PGlu-6 and Au-PTre were similar in performance at the same working concentration, the amount of trehalose was lower in these samples as the bulky PTre allowed less glycopolymer attachment onto the nanoparticle. It can therefore be argued that PGlu-6 is a less effective inhibitor.

The effect of the size of NPs was reevaluated maintaining a constant glycopolymer concentration for the nanoparticles. Free glycopolymers at the same carbohydrate concentration were used as controls. The concentrations were set to PGlu-6: 1.8 μM, PTre: 0.8 μM, respectively, which equated to 0.6 mg mL⁻¹ of the two 62 nm NPs and was adjusted accordingly for the smaller NPs or the free polymers. Upon comparison of equivalent glycopolymer contents, it became evident that the inhibition activity of both glyco-AuNPs was equivalent, whilst the free glycopolymers failed to act as inhibitors (Figure 2d). This result revealed that the inhibition is affected by the glycopolymer concentration and not directly the size of NPs, but the presence of nanoparticles is essential. Similar results were previously reported where linear glucoside polymers showed a lack of binding ability to bacteria, whereas glucose-based polymeric micelles exhibited a remarkable affinity to *E. coli*.^[20] It can be concluded at this stage that

trehalose-based nanoparticles are promising inhibitors of *S. aureus* infection. Nanoparticles based on PGlu-6 still show remarkable activity although it needs to be taken into account that the glycopolymer concentration in each particle is higher due to a higher grafting density.

The measured activity needs to be contrasted to the activity displayed by mannose containing polymers. Here, to achieve 50% inhibition, around 600 μg mL⁻¹ Au₆₂-PTre is required, which equates to a nanoparticle concentration of 0.8 nM or 24.4 μM of trehalose molecules. For comparison, heptyl α-D-mannoside has been identified as an excellent mannose-based inhibitors which is a nanomolar antagonist of FimH.^[56] Bacterial adhesion to epithelial cells was decreased to 22% in the presence of 1 nM (equivalent to 188 nM) heptylmannoside-based glycopolymer while this was decreased to around 70% in the presence of 0.1 nM glycopolymer (equivalent to 18.8 nM mannose).^[57] However, it should be noted the multiplicities of infection (MOI) in our work was 50 which is higher than the aforementioned work (MOI = 10). Other examples include Gold manno-glyconanoparticles as an inhibitor of HIV infection that had IC₅₀ values between 15 and 200 nM per mannose depending on the architecture,^[58] while small molecule α-mannoside inhibitors that prevent adhesion of *E. coli* to HT-29 have IC₅₀ values of around 1 μM.^[59] Although mannose based polymers are still superior, the disadvantage of mannose-based polymers is the large number of competing receptors in the body.

In the next step, the inhibitory role of the 62 nm glyco-AuNPs was investigated by confocal laser scanning microscope (CLSM). To identify the distinctive function of sugar, particularly trehalose, poly(2-hydroxyethyl acrylate) (PHEA) was synthesized to coat Au₆₂NP (ESI, Table S1). As a result of bearing neutral and non-bioactive hydroxyl groups, Au₆₂-PHEA was introduced in the visualization experiments as negative control. Using the aforementioned infection system, HUVECs, labelled with Hoechst 33342, were co-incubated for 2 h with DiD-labeled *S. aureus* in the presence of 62 nm glyco-AuNPs. Unbound bacteria and free NPs were also removed prior to the measurement by CLSM. Non-infected HUVECs and non-treated infected HUVECs were involved as background and control separately. Images were collected after 2 h of incubation (ESI, Figure S13). NPs were observed using the reflective light, which allows quantitative analysis of the interaction of different NPs with cells. Significant cellular uptake of NPs by HUVECs was observed in the case of Au₆₂-PGlu-1, suggesting that the free hydroxyl group on C6 of glucose facilitated the cellular interaction, which effectively removed the NPs from exposure to bacteria. This significantly reduced the inhibitory efficiency of Au₆₂-PGlu-1 and provides a reasonable explanation for its low performance. As shown earlier, the treatment with Au₆₂-PTre led to reduced adhesion compared to other samples. To further emphasize the importance of trehalose as structural feature, another CLSM study was conducted to compare Au₆₂-

Table 1: Molar concentration of nanoparticles and glycopolymers used in the inhibition assay.

Sample AuNPs	Chains per AuNP	Sugars per AuNP	0.15 mg mL ⁻¹		0.3 mg mL ⁻¹		0.6 mg mL ⁻¹	
			[Au] (nM)	[Polymer] (μM)	[Au] (nM)	[Polymer] (μM)	[Au] (nM)	[Polymer] (μM)
Au ₆₂ -PGlu-1	3049	97568		0.3		0.6		1.2
Au ₆₂ -PGlu-6	4449	124572	0.1	0.4	0.2	0.9	0.4	1.8
Au ₆₂ -PTre	2040	61200		0.2		0.4		0.8
Au ₁₆ -PGlu-1	217	6944		1.3		2.6		5.1
Au ₁₆ -PGlu-6	269	7532	5.9	1.6	11.7	3.2	23.5	6.3
Au ₁₆ -PTre	147	4410		0.9		1.7		3.5

PTre with Au₆₂-PHEA. Infected HUVECs with or without NP treatments were fixed followed by staining with Wheat Germ Agglutinin (WGA) and DAPI to label the plasma membrane and nucleic acid separately (Figure 3a). In this case, the invading *S. aureus* were also stained with DAPI, but the nucleic acid belonging to the bacteria and the one belonging to HUVECs could be distinguished by the size as shown by the highlighted bacteria (red circle) in Figure 3a. The DAPI channels show a large number of small bacteria, coexisting with HUVEC cells in the case of the control and Au₆₂-PHEA. The merged channels highlight the co-localization of both. Notably, a lower number of bacteria was observed in the DAPI channel for HUVECs treated with Au₆₂-PTre. This indicates successful infection inhibition as the Au₆₂-PTre treatment prevented bacterial adhesion, resulting in the particles and bacteria being washed away prior to analysis.

To better understand the mechanism of inhibition of glyco-AuNPs, *S. aureus* were fixed onto coverslips and allowed to incubate with NPs for 20 min prior to SEM and TEM analysis (see supporting information). The resulting SEM images (Figure 3b, ESI, Figure S14a) revealed direct binding of Au₆₂-PTre to bacteria in comparison to a lack of interactions for the other nanoparticles. Complementary TEM imaging provided a close-up showing the nanoparticles in close vicinity of the surface in the case of Au₆₂-PTre while no particles were found with the other NP samples (Figure 3b, ESI, Figure S14a). Counting the number of NPs per bacteria revealed the remarkable binding ability of Au₆₂-PTre to *S. aureus* (Figure 3c). Next, the HUVECs were infected with *S. aureus* and treated with Au₆₂-PTre and Au₆₂-PHEA, respectively, for 2 hours (Figure 3d). TEM analysis confirmed that the number of *S. aureus* that has invaded HUVEC was significantly reduced. It was interesting to observe that a few

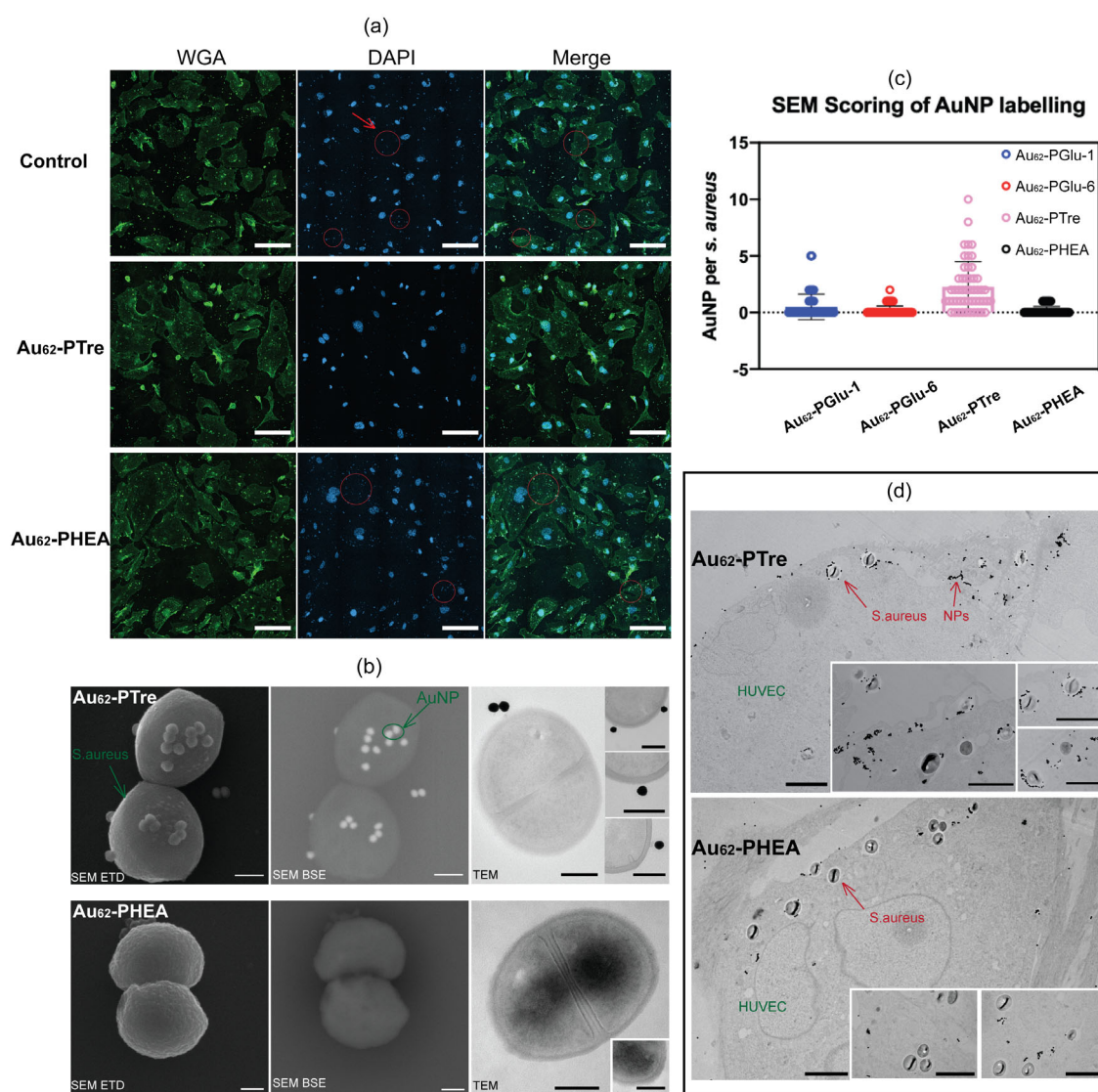


Figure 3. a) CLSM images of infected HUVECs with or without treatment of nanoparticles. (Examples of bacteria was highlighted by labelling) b) SEM and TEM images showing interaction of *S. aureus* with Au₆₂-PTre and Au₆₂-PHEA. c) Quantitative analysis on the binding of nanoparticles with *S. aureus* by SEM. d) TEM images of infective HUVECs with treatment of Au₆₂-PTre and Au₆₂-PHEA. Scale bars equal to 200 μm in (a); 200 nm in (c) and 2 μm in (d).

S. aureus which invaded the cells were still tightly associated with Au₆₂-PTre. This is in contrast to the treatment with Au₆₂-PHEA as the invading *S. aureus* is devoid of any associating Au₆₂-PHEA within HUVECs. Based on Figure 3d, it is proposed that trehalose-functionalized NPs adhere to *S. aureus* hindering the infection efficiency towards HUVECs. Although the majority of bacteria surrounded by trehalose-functionalized nanoparticles were inhibited, a small portion of the bacteria-nanoparticle assembly was taken up by HUVECs by its arrangement on the plasma membrane. As a result, some *S. aureus* may still be able to enter HUVECs, but most likely in a random, non-specific manner. However, the partial inhibition of *S. aureus* by the trehalose-functionalized NPs remains sufficient in affecting colonization.

To further examine the favored binding of trehalose with *S. aureus*, a competitive experiment evaluated by SEM was conducted: *S. aureus* was pre-incubated with free trehalose (40 μM and 400 μM ; 1000- and 10000-fold of PTre) and free glucose (400 μM ; 10000-fold of PTre) for 20 min prior to incubation with Au₆₂-PTre (0.02 nM AuNP; 0.04 μM PTre). Incubation in PBS without added sugar was employed as control sample. Figure 4a shows the SEM images of the resulting interaction between *S. aureus* and Au₆₂-PTre, revealing that decreased binding of nanoparticles to *S. aureus* occurred after pre-treatment with free trehalose. A quantitative analysis based on SEM (Figure 4b) displayed a trehalose-dose dependent disruption on the binding of Au₆₂-PTre to *S. aureus* (ESI, Table S5), while the pretreatment of free glucose at concentration up to 10000-fold of PTre had little effects on disrupting the subsequent binding of Au₆₂-PTre to *S. aureus*. This competitive experiment demonstrated the distinctive role of trehalose as an anti-adhesive in *S. aureus* infection.

While the better activity of PTre is evident, it is still interesting to see that PGlu-6 has a good performance. It is intriguing to think that it is not the attachment of trehalose that causes the anti-adhesive behavior, but simply the presence of glucose connected at 6-position to the polymer. This raises the question if the second glucose unit in PTre might just act as a stiff spacer that directs the binding of

glucose. This could be tested in future work that looks at various glucose-based polymers that contain spacers of various nature between the carbohydrate and the polymer backbone.

In summary, we developed three glyco-AuNPs in two sizes, based on glucose and trehalose glycopolymers. The resulting 62 nm glyco-AuNPs did not present significant toxicity against RAW 264.7 cells and HUVECs at concentration up to 0.75 mg mL⁻¹. The 62 nm NPs were successful to inhibit the *S. aureus* infection to HUVECs albeit failed to inhibit the *P. aeruginosa* infection to HUVECs. Au-PGlu-1 acted less efficient as inhibitor, comparing with Au-PGlu-6 and Au-PTre. This implied the advantageous substitution position of sugar as anti-adhesive. Meanwhile, Au-PGlu-6 and Au-PTre showed the concentration-dependent inhibitory activity. Small sized Au-PGlu-6 and Au-PTre achieved stronger inhibition than the larger AuNPs. However, this difference could be assigned to the presented amount of glycopolymer on the NPs. In this work, two sized trehalose-functionalized NPs displayed impressive inhibition to *S. aureus* infection, with performance surpassing the two glucose-functionalized nanoparticles. The preferential binding of trehalose-functionalized NPs to *S. aureus* was identified by SEM and TEM. This study indicated trehalose as a promising candidate in anti-adhesion treatment. Future work could involve tests with different pathogenic system. In addition, it is also worth exploring if and how trehalose-based therapeutic agents will interfere with the host system.

Acknowledgements

MS would like to thank the Australian Research Council for funding (ARC DP200101918). The authors would like to thank the Mark Wainwright Analytical Centre for their support.

Conflict of Interest

The authors declare no conflict of interest.

Keywords: anti-adhesive agents · bacteria inhibition · glycopolymers · gold nanoparticles · trehalose

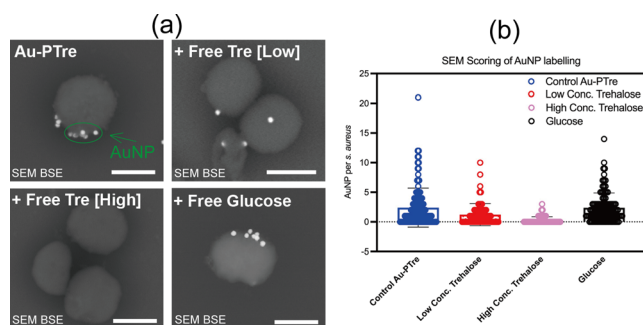


Figure 4. a) SEM images showing *S. aureus* interaction with Au₆₂-PTre with pre-treatment. (Left top: pre-treatment with PBS; right top: pre-treatment with 40 μM free trehalose; left bottom: pre-treatment with 400 μM free trehalose; right bottom: pre-treatment with 400 μM free glucose.) Scale bar equals to 500 nm. b) Quantitative analysis on the binding of nanoparticles per *S. aureus* cell with different pre-treatment by SEM images.

- [1] I. Ofek, D. L. Hasty, N. Sharon, *FEMS Immunol. Med. Microbiol.* **2003**, *38*, 181–191.
- [2] N. Sharon, H. Lis, *Glycobiology* **2004**, *14*, 53R–62R.
- [3] S. Sattin, A. Bernardi, *Trends Biotechnol.* **2016**, *34*, 483–495.
- [4] S. R. S. Ting, G. Chen, M. H. Stenzel, *Polym. Chem.* **2010**, *1*, 1392–1412.
- [5] X. Li, G. Chen, *Polym. Chem.* **2015**, *6*, 1417–1430.
- [6] I. Pramudya, H. Chung, *Biomater. Sci.* **2019**, *7*, 4848–4872.
- [7] M. W. Jones, L. Otten, S.-J. Richards, R. Lowery, D. J. Phillips, D. M. Haddleton, M. I. Gibson, *Chem. Sci.* **2014**, *5*, 1611–1616.
- [8] S. M. Rele, W. Cui, L. Wang, S. Hou, G. Barr-Zarse, D. Tatton, Y. Gnanou, J. D. Esko, E. L. Chaikof, *J. Am. Chem. Soc.* **2005**, *127*, 10132–10133.
- [9] M. A. Mintzer, E. L. Dane, G. A. O’Toole, M. W. Grinstaff, *Mol. Pharm.* **2012**, *9*, 342–354.

- [10] S. Bhatia, L. C. Camacho, R. Haag, *J. Am. Chem. Soc.* **2016**, *138*, 8654–8666.
- [11] F. Lehmann, E. Tiralongo, J. Tiralongo, *Cell. Mol. Life Sci.* **2006**, *63*, 1331–1354.
- [12] K. A. Krogfelt, H. Bergmans, P. Klemm, *Infect. Immun.* **1990**, *58*, 1995–1998.
- [13] T. B. H. Geijtenbeek, D. S. Kwon, R. Torensma, S. J. Van Vliet, G. C. F. Van Duijnhoven, J. Middel, I. L. M. H. A. Cornelissen, H. S. L. M. Nottet, V. N. KewalRamani, D. R. Littman, C. G. Figdor, Y. Van Kooyk, *DC-SIGN, a Dendritic Cell-Specific HIV-1-Binding Protein That Enhances Trans-Infection of T Cells*, Steinman And Inaba, **2000**.
- [14] Y. Guo, H. Feinberg, E. Conroy, D. A. Mitchell, R. Alvarez, O. Blixt, M. E. Taylor, W. I. Weis, K. Drickamer, *Nat. Struct. Mol. Biol.* **2004**, *11*, 591–598.
- [15] Q. Zhang, J. Collins, A. Anastasaki, R. Wallis, D. A. Mitchell, C. R. Becer, D. M. Haddleton, *Angew. Chem. Int. Ed.* **2013**, *52*, 4435–4439; *Angew. Chem.* **2013**, *125*, 4531–4535.
- [16] M. Andreini, D. Doknic, I. Sutkeviciute, J. J. Reina, J. Duan, E. Chabrol, M. Thepaut, E. Moroni, F. Doro, L. Belvisi, J. Weiser, J. Rojo, F. Fieschi, A. Bernardi, *Org. Biomol. Chem.* **2011**, *9*, 5778–5786.
- [17] S. Beloin, A. Barras, F. A. Martin, O. Bande, J.-S. Baumann, J.-M. Ghigo, R. Boukherroub, C. Beloin, A. Siriwardena, S. Szunerits, *Nanoscale* **2013**, *5*, 2307–2316.
- [18] B. D. Polizzotti, K. L. Kiick, *Biomacromolecules* **2006**, *7*, 483–490.
- [19] S. Bhatia, M. Hilsch, J. L. Cuellar Camacho, K. Ludwig, C. Nie, B. Parshad, M. Wallert, S. Block, D. Lauster, C. Böttcher, A. Herrmann, R. Haag, *Angew. Chem. Int. Ed.* **2020**, *59*, 12417–12422; *Angew. Chem.* **2020**, *132*, 12517–12522.
- [20] S. R. S. Ting, E. H. Min, P. B. Zetterlund, M. H. Stenzel, *Macromolecules* **2010**, *43*, 5211.
- [21] L. East, C. M. Isacke, *Biochim. Biophys. Acta Gen. Subj.* **2002**, *1572*, 364–386.
- [22] A. B. Richards, S. Krakowka, L. B. Dexter, H. Schmid, A. P. M. Wolterbeek, D. H. Waalkens-Berendsen, A. Shigoyuki, M. Kurimoto, *Food Chem. Toxicol.* **2002**, *40*, 871–898.
- [23] R. J. Mancini, J. Lee, H. D. Maynard, *J. Am. Chem. Soc.* **2012**, *134*, 8474–8479.
- [24] Y. Liu, J. Lee, K. M. Mansfield, J. H. Ko, S. Sallam, C. Wedemiotis, H. D. Maynard, *Bioconjugate Chem.* **2017**, *28*, 836–845.
- [25] A. Sizovs, L. Xue, Z. P. Tolstyka, N. P. Ingle, Y. Wu, M. Cortez, T. M. Reineke, *J. Am. Chem. Soc.* **2013**, *135*, 15417–15424.
- [26] J. C. Argüelles, *J. Mol. Evol.* **2014**, *79*, 111–116.
- [27] B. Sacktor, *Proc. Natl. Acad. Sci. USA* **1968**, *60*, 1007–1014.
- [28] H. Noll, H. Bloch, J. Asselineau, E. Lederer, *Biochim. Biophys. Acta* **1956**, *20*, 299–309.
- [29] E. Ishikawa, T. Ishikawa, Y. S. Morita, K. Toyonaga, H. Yamada, O. Takeuchi, T. Kinoshita, S. Akira, Y. Yoshikai, S. Yamasaki, *J. Exp. Med.* **2009**, *206*, 2879–2888.
- [30] N. Hao, X. Chen, S. Jeon, M. Yan, *Adv. Healthcare Mater.* **2015**, *4*, 2797–2801.
- [31] X. Chen, B. Wu, K. W. Jayawardana, N. Hao, H. S. N. Jayawardana, R. Langer, A. Jaklenec, M. Yan, *Adv. Healthcare Mater.* **2016**, *5*, 2007–2012.
- [32] S. Srinivasachari, Y. Liu, L. E. Prevette, T. M. Reineke, *Biomaterials* **2007**, *28*, 2885–2898.
- [33] K. M. Mansfield, H. D. Maynard, *ACS Macro Lett.* **2018**, *7*, 324–329.
- [34] A. Piloni, A. Walther, M. H. Stenzel, *Polym. Chem.* **2018**, *9*, 4132–4142.
- [35] M. Nasiri, T. M. Reineke, *Polym. Chem.* **2016**, *7*, 5233–5240.
- [36] A. Miyagawa, R. Tomita, K. Kurimoto, H. Yamamura, *Synth. Commun.* **2016**, *46*, 556–562.
- [37] H. Lu, J. Su, R. Mamdooh, Y. Li, M. H. Stenzel, *Macromol. Biosci.* **2020**, *20*, 1900221.
- [38] S. K. Sahni, *Thromb. Res.* **2007**, *119*, 531–549.
- [39] H. L. Bleich, E. S. Boro, L. Weinstein, J. J. Schlesinger, *N. Engl. J. Med.* **1974**, *291*, 1122–1126.
- [40] M. Ahmed, B. F. L. Lai, J. N. Kizhakkedathu, R. Narain, *Bioconjugate Chem.* **2012**, *23*, 1050–1058.
- [41] J. Lee, E. W. Lin, U. Y. Lau, J. L. Hedrick, E. Bat, H. D. Maynard, *Biomacromolecules* **2013**, *14*, 2561–2569.
- [42] B. J. Spargo, L. M. Crowe, T. Ionedaf, B. L. Beaman, J. H. Crowe, Cord Factor (a,a-Trehalose 6,6'-Dimycolate) Inhibits Fusion between Phospholipid Vesicles (Trehalose/Membrane Fusion/Liposomes/Tuberculosis/Nocardiosis), **1991**.
- [43] S. K. Ogawa, E. R. Yurberg, V. B. Hatcher, M. A. Levitt, F. D. Lowy, *Bacterial Adherence to Human Endothelial Cells In Vitro*, **1985**.
- [44] B. Hara-Kaonga, T. G. Pistole, *J. Microbiol. Methods* **2007**, *69*, 37–43.
- [45] M. Vanaporn, R. W. Titball, *Virulence* **2020**, *11*, 1192–1202.
- [46] J. M. Jeckelmann, B. Erni, *Pfluegers Arch. Eur. J. Physiol.* **2020**, *472*, 1129–1153.
- [47] N. P. Vitko, M. R. Grosser, D. Khatri, T. R. Lance, A. R. Richardson, *MBio* **2016**, *7*, e00296-16.
- [48] V. G. Lewis, M. P. Ween, C. A. Mcdevitt, *Protoplasma* **2012**, *249*, 919–942.
- [49] H. Tournu, A. Fiori, P. Van Dijck, *PLoS Pathog.* **2013**, *9*, e1003447.
- [50] U. Andersson, F. Levander, P. Rådström, *J. Biol. Chem.* **2001**, *276*, 42707–42713.
- [51] S. Khan, N. Cole, E. B. H. Hume, L. L. Garthwaite, T. Nguyen-Khuong, B. J. Walsh, M. D. P. Willcox, *Exp. Eye Res.* **2016**, *151*, 171–178.
- [52] Y. J. Kim, *Acta Crystallogr. Sect. F* **2018**, *74*, 277–282.
- [53] D. Araiza-Olivera, J. G. Sampedro, A. Mújica, A. Peña, S. Uribe-Carvajal, *FEMS Yeast Res.* **2010**, *10*, 282–289.
- [54] F. Liu, J. Liang, B. Zhang, Y. Gao, X. Yang, T. Hu, H. Yang, W. Xu, L. W. Guddat, Z. Rao, *Sci. Adv.* **2020**, *6*, eabb9833.
- [55] A. S. Nouwens, M. D. P. Willcox, B. J. Walsh, S. J. Cordwell, *Proteomics* **2002**, *2*, 1325–1346.
- [56] J. Bouckaert, J. Berglund, M. Schembri, E. De Genst, L. Cools, M. Wührer, C.-S. Hung, J. Pinkner, R. Slättegård, A. Zavialov, D. Choudhury, S. Langermann, S. J. Hultgren, L. Wyns, P. Klemm, S. Oscarson, S. D. Knight, H. De Greve, *Mol. Microbiol.* **2005**, *55*, 441–455.
- [57] A. Sivignon, X. Yan, D. A. Dorta, R. Bonnet, J. Bouckaert, E. Fleury, J. Bernard, S. G. Gouin, A. Darfeuille-Michaud, N. Barnich, *MBio* **2015**, *6*, e01298-15.
- [58] O. Martínez-Ávila, L. M. Bedoya, M. Marradi, C. Clavel, J. Alcamí, S. Penadés, *ChemBioChem* **2009**, *10*, 1806–1809.
- [59] M. Hartmann, H. Papavlassopoulos, V. Chandrasekaran, C. Grabosch, F. Beiroth, T. K. Lindhorst, C. Röhl, *FEBS Lett.* **2012**, *586*, 1459–1465.

Manuscript received: May 15, 2021

Revised manuscript received: July 19, 2021

Accepted manuscript online: August 13, 2021

Version of record online: ■■■■■■, ■■■■■■

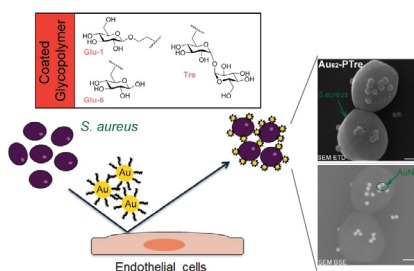
Communications



Glycopolymers

Y. Li, N. Ariotti, B. Aghaei, E. Pandzic,
S. Ganda, M. Willcox, M. Sanchez-Felix,
M. Stenzel*      

Inhibition of *S. aureus* Infection of
Human Umbilical Vein Endothelial Cells
(HUVECs) by Trehalose- and Glucose-
Functionalized Gold Nanoparticles



Due to increased resistance against anti-
biotics, the fight against bacteria
is becoming increasingly difficult. Here, we
used a sugar that is unique to the bacteria
metabolism, trehalose, and prepared tre-
halose-based polymer-coated gold nano-
particles. These nanoparticles were
shown to inhibit the infection of healthy
cells by *S. aureus* and could serve as
a non-toxic alternative to prevent adhe-
sion of certain bacteria.